

A new approach for a Patient-Cooperative Upper Limb FES Support based on Vector Fields^{*}

Arne Passon^{*} Tim Klewe^{*} Thomas Seel^{*} Thomas Schauer^{*}

^{*} *Control Systems Group, Technische Universität Berlin, Einsteinufer 17, EN11, Berlin, Germany (e-mail: passon@control.tu-berlin.de).*

Abstract: Rehabilitation robotics and Functional Electrical Stimulation (FES) are becoming more important in the rehabilitation of stroke and spinal cord injured (SCI) patients. Patient-cooperative control strategies help to only compensate for deficits and to not support too much. The application of a cable-driven arm robotic system with constant force support is considered. FES of the biceps and triceps, as well as of the posterior and anterior part of the deltoid muscle allows us to control the flexion and extension of the elbow joint and of the shoulder motion in the transversal plane. In order to support these motions of the patient, we introduce a novel assist-as-needed FES support based on iterative learning vector fields. Using this new FES control scheme, we aim to facilitate the patient's timing and completion of the motion. The approach is evaluated in experimental trials with healthy subjects performing a breaststroke swimming motion. Starting from a patient-typical deviation of 50°, the controller automatically adapts the support by adjusting the stimulation and thereby reduces the deviation to approximately 15° within less than ten strokes.

© 2017, IFAC (International Federation of Automatic Control) Hosting by Elsevier Ltd. All rights reserved.

Keywords: assist-as-needed, upper limb rehabilitation, multivariable control systems, patient-cooperative, learning control systems, biomedical systems, neuroprosthetics, Functional Electrical Stimulation, rehabilitation robotics

1. INTRODUCTION

Damages of the central nervous system as a result from a stroke or a spinal cord injury (SCI) can lead to a partial or even complete loss of body functions (Popovic and Sinkjaer, 2000). Possible impairments are the loss of hand-, arm- and shoulder functions (Gowland et al., 1992), which handicap the patient to fulfill activities of daily living (ADL). In a lot of these cases, therapy and rehabilitation training can help to prevent muscular atrophy and to train the cardiovascular system. Thereby, the therapy improves the physical condition of the patient in general. For stroke patients, the training can additionally help to relearn lost motor functions. The effectiveness is influenced by the level of challenge (Hogan, 2006), the active participation of the patient (Nelles et al., 2001) as well as by the amount of repetitions and intensity of the training (Kwakkel et al., 1997).

One possibility to enhance these characteristics is to apply Functional Electrical Stimulation (FES) as outlined by Zhang et al. (2007). Peckham and Knutson (2005) for example mention benefits of FES integrated into neuroprostheses for individuals with stroke and SCI.

The development of such a neuroprosthetic system is not straight forward and strongly depends on the task that has to be solved. Model-based approaches, like shown by Riemer (1999), can help to improve the control performance. However, the identification of the models is often difficult, especially if there are many degrees of freedom as in the case of arm movements. Another approach for the training of repetitive movements, as we consider here, is an iterative learning controller design as shown in (Freeman et al., 2015).

1.1 Benefits of Iterative Learning in Arm Movements

An iterative learning design can especially be used to ensure robustness and a good performance without the need for high-order models. It additionally helps to assist as needed by adaptation to the patient's motor abilities, which is one important task in the development of rehabilitation devices to ensure a continuous high initiative and participation of the patient (Emken et al., 2005). However, conventional iterative learning controller (ILC) theory (see e.g. Bristow et al. (2006)) is based on the assumption of a constant pass length (trial duration) and can therefore not be applied to the current application. Only little theory exists that considers the case of a non-uniform trial duration (Seel et al., 2017, 2016; Li et al., 2014). Nevertheless, these ILCs also assume a constant reference which is defined over time. In contrast, we aim for a prespecified movement path without any time restriction. The patient shall be able to freely determine the motion speed. In the research domain of rehabilitation robotics, several other solutions have been

^{*} The work was conducted within the research project BeMobil, which is supported by the German Federal Ministry of Education and Research (BMBF) (FKZ16SV7069K). We would further like to acknowledge Axelgaard Manufacturing Co., USA for donating the used stimulation electrodes. The performed trials have been approved by the ethics committee of the Berlin Chamber of Physicians

proposed. Apart from methods of adaptive control (Wolbrecht et al., 2008), impedance control (Duschau-Wicke et al., 2010a) and the combinations of the two methods (Prez-Ibarra et al., 2015), Duschau-Wicke et al. (2010b) and Guidali et al. (2011) developed control strategies with iteratively learning force fields, which ensure a patient-cooperative support. They all have in common to control the robotics in such a manner that the motion of the patient is guided, but admits space for self-initiative. We only use the robotics to constantly relieve the arm weight and thus solely control the horizontal movements by FES. For this reason, we introduce an adaptation of the approach by Duschau-Wicke et al. (2010b) to FES. We derive a novel patient-cooperative upper limb FES support for horizontal movements based on an iterative learning vector field (ILVF).

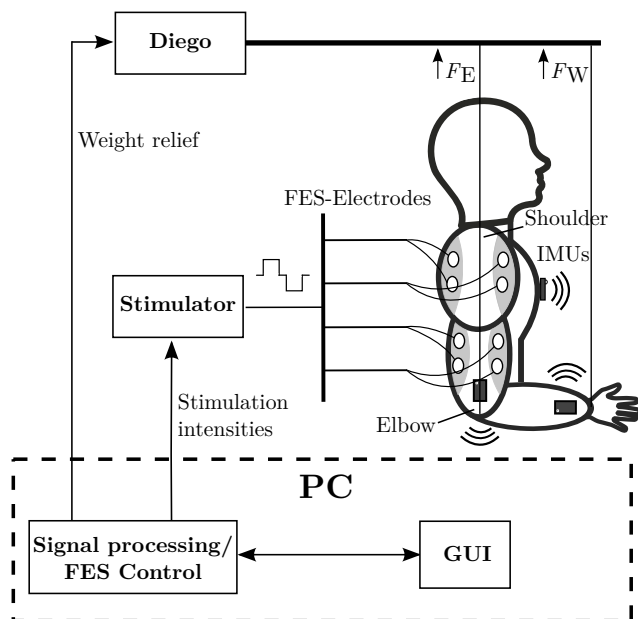


Fig. 1. Experimental setup, here with $F_E = 0$ and $F_W > 0$, i.e. the elbow hangs below the shoulder.

Additionally, for better controllability, we supplemented the controller with an inner co-contraction strategy of the biceps and triceps as suggested by Durfee (1989), which as well produces a more natural activation of the muscles (Hogan, 1984). Thus, it is possible to influence the movement dynamics especially at the moments of braking and turning (Baratta et al., 1988; Hagood et al., 1990).

In summary, this work introduces an ILVF for FES to assist patients while they perform a repetitive arm movement. The motion shall not mandatorily be carried out at a constant speed, but a given trajectory shall be passed completely. Since voluntary muscle recruitment of the patient is not sufficient, the full execution of the motion shall be assured by controlled FES support. Thereby, in the sense of an arm-guiding force field, the assistance shall depend on the distance of the arm to the desired trajectory.

The proposed ILVF for FES is designed in Section 2. The resulting upper limb FES support for repetitive horizontal movements is then evaluated for “dry” breaststroke swimming motions of healthy subjects in Section 3.

2. METHODS

Experiments were performed as shown in Fig. 1 with a stimulation system (RehaStim, Hasomed GmbH, Germany), the active cable-driven robotic system DIEGO (Tyromotion GmbH, Austria), three wireless inertial measurement units (IMUs) (MTwTM, Xsens, Netherlands) and a PC running Linux. A soft real-time system with a sampling rate of 100 Hz runs the control algorithms and processes the IMU data, while the stimulation frequency is chosen at 25 Hz and the robotics communicates at 20 Hz. The software is implemented using Simulink[®] and a modified Linux real-time target (Sojka and Pisa (2014)) is employed to generate the code and to provide a network communication to a Python-GUI.

Two ropes of the robotics are attached to the forearm, where one is connected next to the elbow joint and the other next to the wrist joint. The actuators are located above the user and thus the directions of the ropes depend on the current upper limb position related to the actuators. Forces with the magnitudes F_W at the wrist and F_E at the elbow are applied at these ropes to realize a weight support. They are chosen in such a way that the subject’s elbow and wrist are levitating on the same level as the shoulder.

The intensity-controlled (subject-dependent current $I=10$ – 50 mA, pulse width $pw=0$ – 500 μ s) stimulation impulses are applied through self-adhesive hydro-gel electrodes. Thereby, the stimulation intensity $q \in [0, 1]$ is equally distributed on the ranges of the current I and the pulse width pw as described in (Klauer et al., 2012). The shoulder flexion and extension in the transversal plane is achieved by the stimulation of the posterior and anterior part of the deltoid muscle. FES of the biceps and triceps produce flexion and extension of the elbow joint.

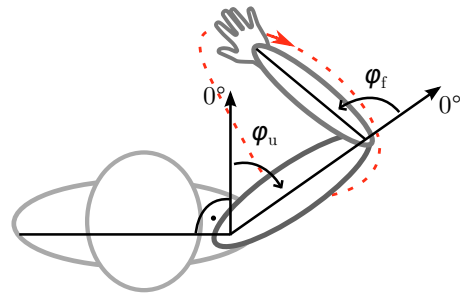


Fig. 2. Geometry of the upper limbs with the estimated angles of the upper arm φ_u and forearm φ_f .

The IMUs are placed on the forearm, upper arm and chest as shown in Fig. 1. The shoulder angle in the transversal plane φ_u and the elbow angle φ_f are then estimated using orientation estimates (see Seel and Ruppig (2017)) of the three IMUs. The geometric setting is illustrated in Fig. 2.

2.1 Control Idea

The idea of the vector field is, as depicted in Fig. 3, that each arm position can be considered as a point on a field, the domain of which is spanned by the two arm angles φ_u and φ_f . The currently measured position of the arm can then be taken to obtain the vector to the nearest neighbor

of a given reference trajectory. The advantage is, that thus an only position-based and not time-dependent error is achieved. This error vector consists of the two errors for the separated controller paths of the two joints. However, the controllers of forearm and upper arm as well as the initial vector field only consist of proportional gains and thus steady-state errors will remain. To counteract this, the remaining errors of the current cycle are collected and an iterative learning law updates the vector field each time a cycle is finished. An integration of the errors in the vector field takes place from cycle to cycle in order to increase the FES support if required.

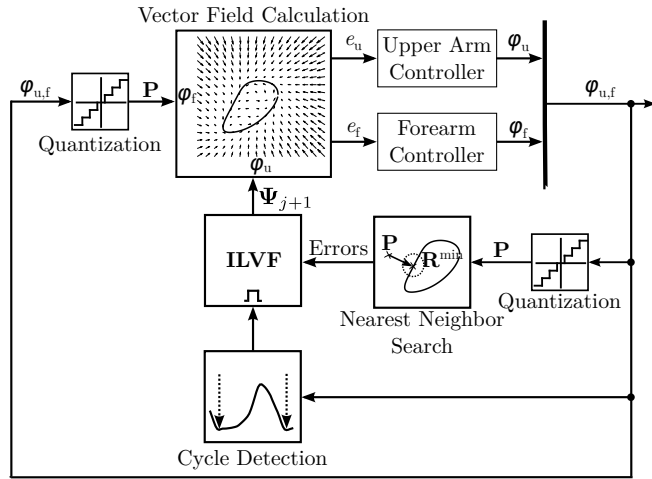


Fig. 3. Iterative learning vector field with the nearest-neighbor search (see Fig. 6), which generates the five errors depending on the measured position \mathbf{P} and its nearest neighbor \mathbf{R}^{\min} . Each cycle j determines an adapted vector field Ψ_{j+1} which maps the current position to the errors e_u and e_f for the upper arm and forearm controllers (see Fig. 5).

2.2 Separated Control Paths and Composition of the Antagonistic Muscle Pairs

The antagonistic muscle pairs are both assumed to be single input systems due to the concurrent influence of both muscles on the belonging joint angle and to achieve a shared control input. For this purpose, the deltoid muscle pair is treated by a split range controller as shown in Fig. 4, where the control signal of the upper arm $u_u \in [-1, 1]$ is actuating the anterior deltoid in the range of $[-1, 0]$ with the normalized stimulation intensity $\hat{q}_{u,a} = |u_u|$. In this context, normalized stimulation intensity means, that it is normalized between the subject dependent threshold $q_{u,a}^{\text{thr}}$, which is necessary to produce a visible movement and the maximum tolerated intensity $q_{u,a}^{\text{max}}$. Respectively the posterior deltoid is actuated in the range of $(0, 1]$ with $\hat{q}_{u,p} = u_u$.

A simple split range controller for the elbow joint has led to partly jerky motions, which especially occurred at the moments of braking and turning. Durfee (1989) demonstrated the potential of co-contraction of antagonistic muscle pairs to enhance the joint angle control. We decided to implement such a co-contraction strategy for the biceps and triceps. Zhou et al. (1996) examined

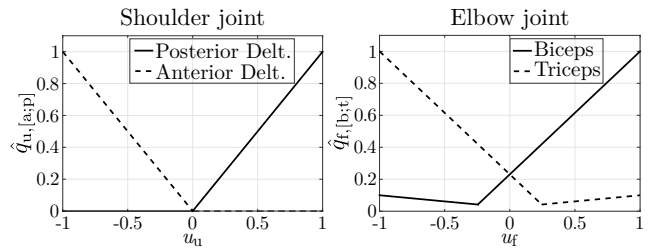


Fig. 4. Composition of the normalized stimulation intensities of the shoulder joint $\hat{q}_{u,[a;p]}$ (split range control) and elbow joint $\hat{q}_{f,[b;t]}$ (co-contraction with an overlap of 30% and an antagonist gain of 10%).

three types of co-contraction strategies. The combined co-contraction strategy with an overlap and an antagonist gain showed the best results. An overlap of 30% and an antagonist gain of 10% as shown in Fig. 4 revealed the smoothest trajectories in our tests when controlling the joint angle manually using u_f as input.

The resulting separated control paths of each joint, which are completed by a proportional gain of the forearm $K_{p,f}$ and upper arm $K_{p,u}$ are depicted in Fig. 5. Inputs are the errors e_f and e_u respectively.

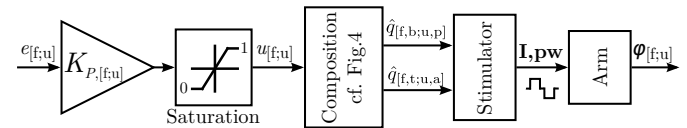


Fig. 5. Separated control paths for the angles φ_f and φ_u respectively.

2.3 Vector Field

Based on the concept by Duschau-Wicke et al., the errors of the forearm e_f and upper arm e_u shall now be generated by a vector field. The joint angle of the forearm φ_f as y-axis and the upper arm angle φ_u as x-axis span the domain of the vector field. Real-time capability is ensured by a quantization of the vector field with a resolution of $\Delta\varphi = 2.5^\circ$ and by a limitation of the ranges of both axes from $\varphi^{\min} = -30^\circ$ to $\varphi^{\max} = 120^\circ$, which is normally not exceeded in rehabilitation movements. The minimal distance of each quantized position $\mathbf{P} = [\varphi_u^q \ \varphi_f^q]^T$ in the vector field to a given reference trajectory $\mathbf{R} \in \mathbb{R}^{2 \times l_R}$ consisting of l_R equidistant points is calculated using the Euclidean norm. Thus, the minimal distance vector for each \mathbf{P} is given by

$$\mathbf{D} = \mathbf{R}^{\min} - \mathbf{P} \quad \text{with} \quad \mathbf{R}^{\min} = \arg \min_{\mathbf{R}(:,k)} \|\mathbf{R}(:,k) - \mathbf{P}\|_2, \quad k = 1 \dots l_R. \quad (1)$$

The desired movement direction thereby corresponds to increasing values of k .

Smooth movement transitions from an undesired position to the reference trajectory are achieved by twisting \mathbf{D} into the direction of motion. Therefore, a forward-looking vector

$$\mathbf{F} = \mathbf{R}(:, k_{\min} + k_f) - \mathbf{R}^{\min} \quad (2)$$

is determined using $\mathbf{R}^{\min} = \mathbf{R}(:, k_{\min})$. The forward-looking number k_f specifies the number of sampling points

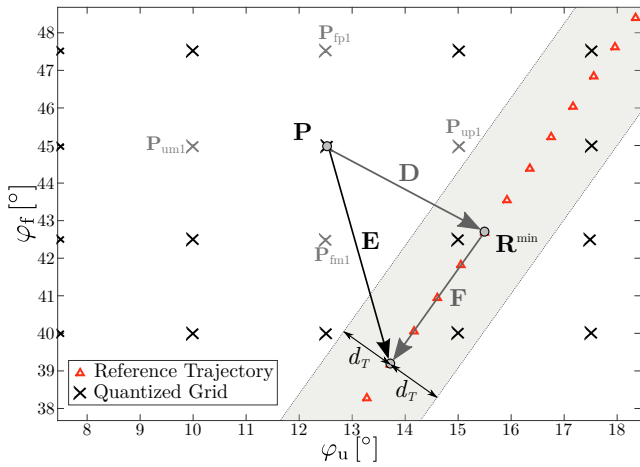


Fig. 6. Nearest-neighbor search and calculation of the error vector \mathbf{E} depending on the nearest neighbor \mathbf{R}^{\min} , the forward-looking vector \mathbf{F} and the tunnel radius d_T .

on the reference trajectory to look ahead. Thus, the twisted distance vector is given by

$$\mathbf{D}_F = \mathbf{D} + \mathbf{F}. \quad (3)$$

An additional propulsion on the reference trajectory itself can be obtained by the supplement of a tunnel with a radius d_T around the target trajectory. Error vectors inside this tunnel are normalized to a tunnel propulsion length T_{norm} . Thus, it is possible to independently increase the speed inside the tunnel if a patient is not able to achieve a desired voluntary propulsion. The constant propulsion inside the tunnel moreover enhances the smoothness of the desired movement. Consequently, each element \mathbf{E} of the initial error vector field is calculated as

$$\mathbf{E} = \begin{cases} \mathbf{D}_F & \text{if } \|\mathbf{D}\|_2 \geq d_T \\ T_{\text{norm}}(\mathbf{D}_F / \|\mathbf{D}_F\|_2) & \text{if } \|\mathbf{D}\|_2 < d_T. \end{cases} \quad (4)$$

Fig. 6 explains the calculation of one exemplary \mathbf{E} , whereby it should be noted that the four surrounding grid points $\mathbf{P}_{\text{fm}1}$, $\mathbf{P}_{\text{fp}1}$, $\mathbf{P}_{\text{um}1}$ and $\mathbf{P}_{\text{up}1}$ are only taken into account during the iterative learning and for this reason will be explained in Section 2.4.

The initial error vector field Ψ_0 is then determined by

$$\Psi_0(i_u, i_f) = \mathbf{E}(\mathbf{P}(\varphi_u^q, \varphi_f^q)), \quad (5)$$

where the position index of the shoulder joint is calculated as

$$i_u = \frac{\varphi_u^q - \varphi_u^{\min}}{\Delta\varphi} \quad \forall \varphi_u^q \in [\varphi_u^{\min}, \varphi_u^{\min} + \Delta\varphi, \dots, \varphi_u^{\max}],$$

and i_f is calculated analogously.

However, up to now, the presented control algorithm only includes proportional gains and thus a steady-state error will remain. Hence, after each finished breaststroke cycle with index j , the initial Ψ_0 has to be adjusted by iterative learning to reduce the remaining error.

2.4 Iterative Learning of the Vector Field

Run-Time Error Collection The iterative learning vector field shall adjust the errors of all passed points during run-time. Though, the errors inside the tunnel with radius d_T shall not be changed. Thus, small deviations from the reference are discarded. Additionally the propulsion on

the target trajectory itself is not changed, since up to now it is not planned to iteratively adapt the subject's speed on the reference. The four surrounding grid points $\mathbf{P}_{\text{fm}1}$, $\mathbf{P}_{\text{fp}1}$, $\mathbf{P}_{\text{um}1}$ and $\mathbf{P}_{\text{up}1}$ of a passed point \mathbf{P} are additionally taken into account for the error adaptation. These virtual actual positions extend the learning area and hence facilitate the reaction to potentially slightly different follow-up trajectories. Thus, the algorithm memorizes five positions in each sampling step, which is a chosen trade-off due to the necessary real-time capability.

Consequently, an error vector matrix of the current cycle j , which is a zero matrix at the beginning of the cycle, is determined by

$$\mathbf{E}_j(i_u, i_f) = \Psi_0(i_u, i_f) \quad \text{if } \|\mathbf{D}(i_u, i_f)\|_2 > d_T \quad (6)$$

for all pairs (i_u, i_f) belonging to passed points as well as the four surrounding grid points. \mathbf{E}_j is then used by the iterative learning procedure when it is triggered by a finished cycle, to increase the FES for any passed points outside the tunnel.

Cycle Detection The iterative learning procedure has to be triggered once a cycle of the repetitive movements is completed. Consequently, a cycle detection is necessary, which depends on the movement pattern. We consider periodic breaststroke motions in this case and thus a minimum search over the last six samples of the distance to the vector field origin yields applicable results. Thus, a finished cycle is detected after the arm position passed the furthest frontal stretching during the cycle as visible in Fig. 2.

Iterative Learning Algorithm Using the collected new error vectors of the last cycle from (6), the iterative learning algorithm adapts the vector field each time it is triggered by the cycle detection. We use the actual error cycle matrix \mathbf{E}_j and the latest vector field Ψ_j to obtain the vector field of the next cycle by using the following learning law:

$$\Psi_{j+1} = (1 - \gamma) \Psi_j + \lambda \mathbf{E}_j + \gamma \Psi_0, \quad (7)$$

where $\lambda \in \mathbb{R}_{\geq 0}$ is an adjustable learning gain. The also adjustable forgetting factor $\gamma \in [0, 1)$ slightly decrements the support in the next cycle if an error has not been occurred and thus demands the subject to be proactive. In this way, as advised in (Duschau-Wicke et al., 2010b) and (Emken et al., 2005) an assist-as-needed system is ensured. The supplement of the γ -multiplied Ψ_0 guarantees that the initial vector field is never forgotten and thus especially areas which are not yet passed are not changed. The forgetting factor additionally limits the maximal magnification of continuously updated error vectors to $\lambda/\gamma + 1$ if $\gamma > 0$.

The resulting ILVF control system with the current vector field Ψ_j , which takes the actual position \mathbf{P} as input and generates the outputs e_f and e_u for the separated controller paths of forearm and upper arm, is shown in Fig. 3.

3. EXPERIMENTAL VALIDATION

The designed ILVF scheme is now evaluated in experimental trials with four healthy subjects (age of 25-27 years). As mentioned before, the subjects had to perform a breaststroke motion in the air. They did not see any reference and were instructed to realize the swimming movements

with minimal effort and as fast as they wanted while not operating against the FES. Thus, the most comparable conditions to patients' behavior were achieved. The subjects had to accomplish 20 cycles without FES, 20 with the initial vector field Ψ_0 and then 20 with the ILVF, always with a suitable weight relief by the rehabilitation robotic system DIEGO. Afterwards, the sequence is repeated once.

A reference trajectory was generated from recorded breaststroke movements of six healthy subjects (age of 25-30 years) using the setup as described in Section 2, with no FES applied. As a side product from the additionally recorded Electromyograms (EMGs) of the later stimulated muscles, the voluntary co-contraction of the two muscle pairs was visible, which moreover confirmed the use of co-contraction for the FES of the elbow joint. The around 50 cycles of each subject were first independently averaged to six mean breaststroke movements. The six generated means of each subject were then collectively averaged to obtain the resulting reference.

The initial Ψ_0 is then determined using this reference and $k_F = 10$, $d_T = 5$ and $T_{\text{norm}} = 20$, which turned out from our first trials as good initial vector field settings. Following literature (Seel et al., 2016; Duschau-Wicke et al., 2010b) and as well based on first experiences, the learning gain and forgetting factor of the ILVF were chosen as $\lambda = 0.4$ and $\gamma = 0.1$. The co-contraction parameters of the elbow joint are determined by an overlap of 30% and an antagonist gain of 10% as described in Section 2.2. The proportional gain of the forearm $K_{p,f} = 0.01$ and upper arm $K_{p,u} = 0.02$ were chosen from first trial experiences at which the upper arm needed a stronger gain due to its higher inertia.

The completed setup was then used to implement the defined ILVF on a soft real-time computer system. At first, the stimulation thresholds $q_{u,[a;p]}^{\text{thr}}$ and $q_{f,[b;t]}^{\text{thr}}$ as well as the maximum tolerated stimulation intensities $q_{u,[a;p]}^{\text{max}}$ and $q_{f,[b;t]}^{\text{max}}$ of each subject were detected. The intensities were increased until a minimal motion was detected to assign the thresholds and was then further increased until the subjects reported discomfort to set the maximums. Then the two sequences of breaststroke motions as described above started.

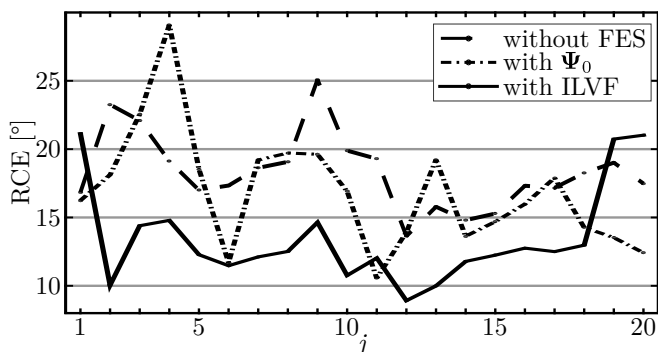


Fig. 7. Relative cycle error (RCE) of the first sequence of a healthy subject (S4-2 in Table A.1) for a generated ordinary breaststroke reference.

We investigate whether the proposed ILVF can automatically optimize the initial vector field Ψ_0 so that the

deviations from the reference decrease. For this reason, we calculated a relative cycle error (RCE) as the root-mean-square of the euclidean norm of all error vectors of one breaststroke swimming cycle. Fig. 7 shows representative results of one sequence of the subject 4 (c.f. S4-2 in Table A.1). The ILVF is able to hold the RCE mostly between 10-15°, which is a good tracking for the naturally varying breaststroke motion. Higher tracking accuracies will hardly be achieved due to the natural fluctuation of the FES influences and the high freedom of movement in the DIEGO. Since the subjects are healthy, the voluntary movements without FES are already not so far away from the desired trajectory, which is as well visible in the exemplary result shown in Fig. 8. As a result, a good evaluation between the different supports is difficult as the RCEs at the top of Table A.1 and the box plot of all subjects in Fig. A.1 indicate.

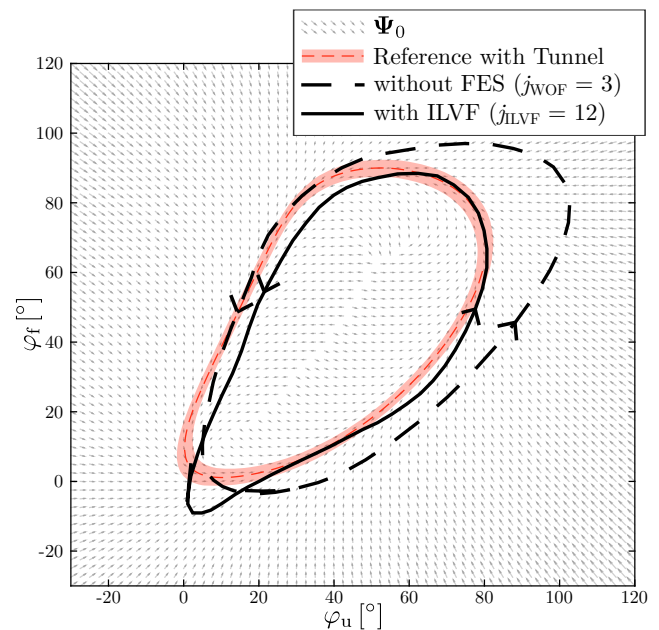


Fig. 8. Exemplary results of a healthy subject (S4-2 in Table A.1).

To be able to achieve a reliable validation also with healthy subjects, the reference is then scaled down to an unnatural breaststroke motion $r_{\text{scale}} = [25^\circ 45^\circ]$ and thus a high deviation of the voluntary movement is obtained as depicted in Fig. 9. A decreasing tendency of the RCE is achieved when the ILVF is active. Furthermore, an increasing tendency of the RCE arose using the initial vector field (VF= Ψ_0), potentially evoked by muscle fatigue. Adapting the support to the arising muscle fatigue, the iterative learning system could quite likely prevent the increasing error to a certain extent. The exemplary results in Fig. 10 with the smaller reference clearly demonstrate the possible enhancements in case of stronger deviations.

The RCEs of the two subjects with whom the trials were repeated are given at the bottom of Table A.1. The improvement by the ILVF in comparison with the support by the non-adapting initial vector field becomes particularly obvious in the corresponding box plots in Fig. A.2.

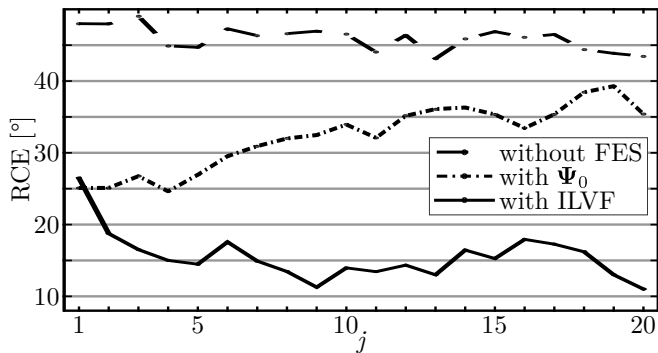


Fig. 9. Relative cycle error (RCE) of the second sequence of small breaststroke motions of a healthy subject (S4-s in Table A.1).

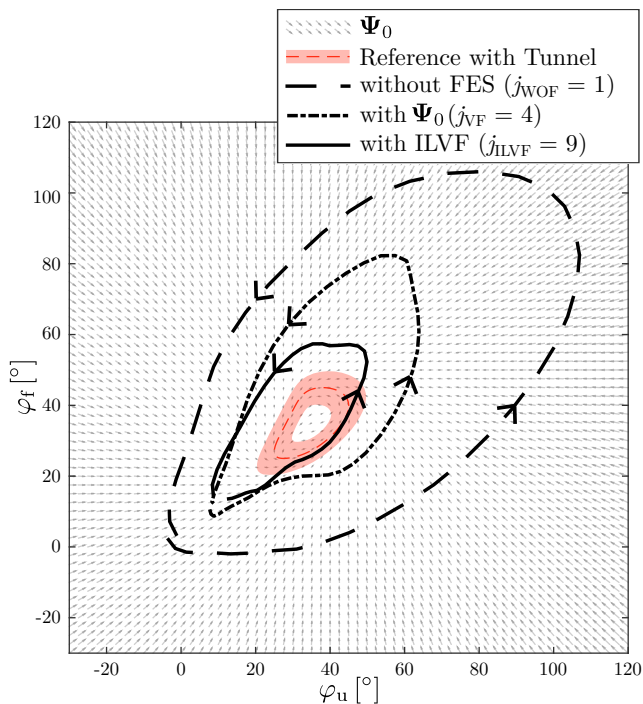


Fig. 10. Exemplary results of a healthy subject (S4-s in Table A.1) for a scaled-down breaststroke reference.

4. CONCLUSIONS AND FURTHER RESEARCH

To our best knowledge, this is the first time that an ILVF for FES is designed. We are still at the beginning of the development and have not yet investigated the influences of all parameters in full detail. The tuning of the parameters has been done by trial and error. Thus, the results spread a lot and vary from subject to subject. Proper theory to choose the parameters and to analyze the performance of the system needs to be developed. For this reason, we are currently developing a model of the upper arm including the forces imposed by the rehabilitation robotics DIEGO to further evaluate the proposed methods. The influence of the motion speed is not yet taken into account and could especially be included to consider the known delayed muscle contraction by FES. A therapy-task-depending adaptation of the support within the tunnel is another future objective. Experimental trials with stroke and spinal cord injured patients shall also be

performed. The approach nevertheless already shows the potential for FES support of repetitive motions based on vector fields. It could particularly be applied for the rehabilitation of the upper limb in combination with robotics as described in (Guidali et al., 2011) or passive exoskeletons as used in (Klauer et al., 2013).

ACKNOWLEDGEMENTS

We would like to express our most sincere gratitude to the subjects of our experiments.

REFERENCES

- Baratta, R., Solomonow, M., Zhou, B., Letson, D., Chuinard, R., and D'Ambrosia, R. (1988). Muscular coactivation: The role of the antagonist musculature in maintaining knee stability. *The American Journal of Sports Medicine*, 16(2), 113–122.
- Bristow, D.A., Tharayil, M., and Alleyne, A.G. (2006). A survey of iterative learning control. *IEEE Control Systems*, 26(3), 96–114.
- Durfee, W.K. (1989). Task-based methods for evaluating electrically stimulated antagonist muscle controllers. *IEEE Transactions on Biomedical Engineering*, 36(3), 309–321.
- Duschau-Wicke, A., Zitzewitz, J.v., Caprez, A., Lunenburger, L., and Riener, R. (2010a). Path Control: A Method for Patient-Cooperative Robot-Aided Gait Rehabilitation. *IEEE Transactions on Neural Systems and Rehabilitation Engineering*, 18(1), 38–48.
- Duschau-Wicke, A., Andr, M., Vallery, H., and Riener, R. (2010b). Adaptive Patientenunterstützung für Rehabilitationsroboter. *Automatisierungstechnik*, 58(5), 260–268.
- Emken, J.L., Bobrow, J.E., and Reinkensmeyer, D.J. (2005). Robotic movement training as an optimization problem: designing a controller that assists only as needed. In *9th International Conference on Rehabilitation Robotics, 2005. ICORR 2005.*, 307–312.
- Freeman, C., Rogers, E., Burrige, J., Hughes, A., and Meadmore, K. (2015). *Iterative Learning Control for Electrical Stimulation and Stroke Rehabilitation*. Springer London.
- Gowland, C., deBruin, H., Basmajian, J.V., Plews, N., and Burcea, I. (1992). Agonist and Antagonist Activity During Voluntary Upper-Limb Movement in Patients with Stroke. *Physical Therapy*, 72(9), 624–633.
- Guidali, M., Schlink, P., Duschau-Wicke, A., and Riener, R. (2011). Online learning and adaptation of patient support during ADL training. In *2011 IEEE International Conference on Rehabilitation Robotics*, 1–6.
- Hagood, S., Solomonow, M., Baratta, R., Zhou, B., and D'Ambrosia, R. (1990). The effect of joint velocity on the contribution of the antagonist musculature to knee stiffness and laxity. *The American Journal of Sports Medicine*, 18(2), 182–187.
- Hogan, N. (1984). Adaptive control of mechanical impedance by coactivation of antagonist muscles. *IEEE Transactions on Automatic Control*, 29(8), 681–690.
- Hogan, N. (2006). Motions or muscles? Some behavioral factors underlying robotic assistance of motor recovery. *Journal of Rehabilitation Research & Development*, 43(5), 605–618.

- Klauer, C., Raisch, J., and Schauer, T. (2012). Linearisation of electrically stimulated muscles by feedback control of the muscular recruitment measured by evoked emg. In *Proc. of the 17th International Conference on Methods and Models in Automation and Robotics, IEEE*, 108–113. Midzysdroje, Poland.
- Klauer, C., Raisch, J., and Schauer, T. (2013). Nonlinear joint-angle feedback control of electrically stimulated and lambda-controlled antagonistic muscle pairs. In *European Control Conference (ECC), 2013*, 3101–3107.
- Kwakkel, G., Wagenaar, R.C., Koelman, T.W., Lankhorst, G.J., and Koetsier, J.C. (1997). Effects of Intensity of Rehabilitation After Stroke. *Stroke*, 28(8), 1550–1556.
- Li, X., Xu, J.X., and Huang, D. (2014). An iterative learning control approach for linear systems with randomly varying trial lengths. *IEEE Transactions on Automatic Control*, 59(7), 1954–1960.
- Nelles, G., Jentzen, W., Jueptner, M., Mller, S., and Diener, H.C. (2001). Arm Training Induced Brain Plasticity in Stroke Studied with Serial Positron Emission Tomography. *NeuroImage*, 13(6), 1146 – 1154.
- Peckham, P.H. and Knutson, J.S. (2005). Functional Electrical Stimulation for Neuromuscular Applications. *Annual Review of Biomedical Engineering*, 7(1), 327–360.
- Popovic, D. and Sinkjaer, T. (2000). *Control of Movement for the Physically Disabled*. Springer, 1 edition.
- Prez-Ibarra, J.C., Siqueira, A.A.G., and Krebs, H.I. (2015). Assist-as-needed ankle rehabilitation based on adaptive impedance control. In *2015 IEEE International Conference on Rehabilitation Robotics (ICORR)*, 723–728.
- Riener, R. (1999). Model-based development of neuro-prosthesis for paraplegic patients. *Philosophical Transactions of the Royal Society B: Biological Sciences*, 354(1385), 877–894.
- Seel, T. and Ruppig, S. (2017). Eliminating the Effect of Magnetic Disturbances on the Inclination Estimates of Inertial Measurement Units. In *IFAC World Congress 2017 (submitted)*.
- Seel, T., Schauer, T., and Raisch, J. (2017). Monotonic convergence of iterative learning control systems with variable pass length. *International Journal of Control*, 90(3), 393–406.
- Seel, T., Werner, C., and Schauer, T. (2016). The adaptive drop foot stimulator – Multivariable learning control of foot pitch and roll motion in paretic gait. *Medical Engineering & Physics*, 38(11), 1205 – 1213.
- Wolbrecht, E.T., Chan, V., Reinkensmeyer, D.J., and Bobrow, J.E. (2008). Optimizing Compliant, Model-Based Robotic Assistance to Promote Neurorehabilitation. *IEEE Transactions on Neural Systems and Rehabilitation Engineering*, 16(3), 286–297.
- Zhang, D., Guan, T.H., Widjaja, F., and Ang, W.T. (2007). Functional Electrical Stimulation in Rehabilitation Engineering: A Survey. In *Proceedings of the 1st International Convention on Rehabilitation Engineering & Assistive Technology*, 221–226. New York, USA.
- Zhou, B.H., Baratta, R.V., Solomonow, M., Olivier, L.J., Nguyen, G.T., and D’Ambrosia, R.D. (1996). Evaluation of isometric antagonist coactivation strategies of electrically stimulated muscles. *IEEE Transactions on Biomedical Engineering*, 43(2), 150–160.

Appendix A. COMPLEMENTARY RESULTS

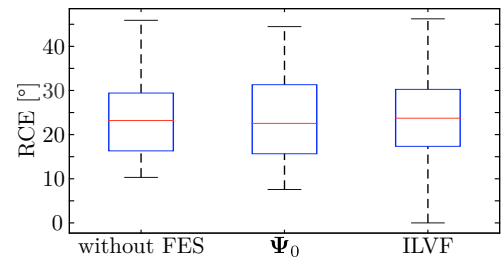


Fig. A.1. Box plot of the relative cycle errors (RCEs) of all subjects for a generated ordinary breaststroke reference.

Table A.1. Mean relative cycle errors (RCEs) in degree of four healthy subjects S1-S4 for the normal (S1 - S4-2) and small (S2-s and S4-s) breaststroke reference with their standard deviations of each session and in total, where 'w/o' means without FES. Entries declared as 'x' were lost during data transfer and thus denoted with '*' only consists of 16-18 recorded cycles, the others of 20 cycles.

Subject	Method	Sequence					
		1		2		total	
		mean	σ	mean	σ	mean	σ
S1	w/o	31.4	4.8	x	x	31.4	4.8
	Ψ_0	32.6	2.9	32.1	3.5	32.4	3.2
	ILVF	27.0	7.9	25.9	5.1	26.4	6.5
S2	w/o	x	x	34.0	4.4	34.0	4.4
	Ψ_0	34.6	4.6	31.6*	4.2	33.2	4.6
	ILVF	33.6	8.7	36.6	4.5	35.1	7.0
S3	w/o	27.6*	2.6	19.1	2.4	22.8	4.9
	Ψ_0	22.9*	1.8	21.3*	2.1	22.2	2.0
	ILVF	25.1	1.8	21.7	2.1	23.2	2.7
S4-1	w/o	13.1	1.3	16.0	2.1	14.6	2.3
	Ψ_0	10.5	2.3	15.4	2.9	12.9	3.6
	ILVF	12.9	1.9	x	x	12.9	1.8
S4-2	w/o	18.3	2.8	27.2	2.7	22.7	5.2
	Ψ_0	16.9	4.2	17.1	3.7	17.0	3.9
	ILVF	13.5	3.6	22.2*	6.6	17.6	6.8
S2-s	w/o	40.0	1.4	x	x	40.0	1.3
	Ψ_0	21.1	2.5	30.6	1.7	25.9	5.2
	ILVF	18.2	3.9	21.8	4.1	20.0	4.4
S4-s	w/o	43.7	1.4	45.9	1.6	44.8	1.9
	Ψ_0	27.9	2.7	32.2	4.5	30.1	4.3
	ILVF	20.4	4.1	15.5	3.3	18.0	4.5

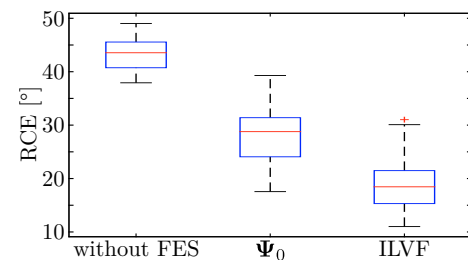


Fig. A.2. Box plot of the relative cycle errors (RCEs) of both subjects for a generated small breaststroke reference.